Shock Capturing with Discontinuous Galerkin Method

Vinh Tan NGUYEN[1], **Boo Cheong KHOO**[1,2], **Jaime PERAIRE**[1,3] and Per-Olof PERSSON[3]

[1] Singapore-MIT Alliance
[2] Department of Mechanical Engineering, National University of Singapore
[3] Department of Aeronautics and Astronautics, Massachusetts Institute of Technology

Abstract—**Shock capturing has been a challenge for computational fluid dynamicists over the years. This article deals with discontinuous Galerkin method to solve the hyperbolic equations in which solutions may develop discontinuities in finite time. The high order discontinuous Galerkin method combining the basis of finite volume and finite element methods has shown a lot of attractive features for a wide range of applications. Various techniques proposed in the literature to deal with discontinuities basically reduce the order of interpolation in the region around these discontinuities. The accuracy of the scheme therefore may be degraded in the vicinity of the shock. The proposed method resolves the discontinuities presented in the solution by applying viscosity into the shock-containing elements. The discontinuity is spread over a distance and is well approximated in the space of interpolation functions. The technique of adding viscosity to the system and the indicator based on the expansion coefficients of the solution are presented. A number of numerical examples in one and two dimensions is carried out to show the capability of the scheme for shock capturing.**

Index Terms—**Discontinuous Galerkin method, indicator, limiter, shock capturing.**

I. Introduction

Discontinuous Galerkin method has been widely used in computational fluid dynamics for the past few decades. Since then it has been attracting the interest of many researchers in putting efforts to develop approaches to solve the problems involving shocks and discontinuities. It is well-known that the solutions to the non-linear PDEs may develop discontinuities in finite time and present very complicated structure near such discontinuities. It has also been shown that the discontinuous Galerkin method is capable of solving these kinds of problem by using a suitable limiting techniques to resolve the discontinuities [2], [3], [4], [5].

Essentially, the stability condition is not satisfied by the DG space discretization method itself and it is therefore necessary to enforce stability of the scheme via the limiters. In general, as the solution develops discontinuities it has to be limited to prevent oscillations from overwhelming the solution. A number of approaches has been developed to limit the solutions with some acceptable results; however there are some limitations involved. The most commonly used technique reduces the order of the approximation in the elements that are identified to contain the discontinuities by using some indicators [1]. An amount of dissipation is then added to the DG method by reducing the order of interpolation in the shock region. It has been shown that this arrangement is able to resolve the shock

with an acceptable result especially when it is combined with adaptive mesh refinement technique [9]. On the other hand, the accuracy of the method may be affected by the flattening of the solution in the vicinity of the discontinuities and the problem in higher dimensional problem has not been well resolved. Designing an appropriate indicator is another issue in limiting the solution but still a lot of techniques have been developed in the literature [7] for the purpose of identifying the trouble cells. In [1] a simple indicator, slope limiter, is introduced and has shown to be a good choice to detect the shocks. A major disadvantage of this algorithm is that the accuracy of the solution may be degraded due to the treatment applied across the shock. In fact the solution in the vicinity of the shock is only first order accurate. Alternatively, a high order non-oscillatory reconstruction scheme, WENO has been used as a limiter in DG and shown to be an alternative choice [6]. However, this high order reconstruction based limiter requires a very wide stencil and therefore the compactness of DG may becomes less attractive. One may refer to [7] for a review of the various indicators used in literature.

A simple technique which uses viscosity to resolve the discontinuities within a cell is proposed in this work. It is inspired from previous artificial viscosity methods [10] proposed in the earlier work by Von Neumann and Richmyer. The idea of adding viscosity is to spread the discontinuity over a length scale so that it can be resolved in the space of interpolating functions. In general the resolution given by a piecewise polynomials of order p scales like $\delta \sim h/p$. Hence the amount of viscosity required to resolve a shock is of order $\mathcal{O}(h/p)$. Comparing to the previous methods of resolving the shocks which is of order $\mathcal{O}(h)$, the accuracy of the solution is $\mathcal{O}(h/p)$ in the vicinity of the shock. This means that the higher order of polynomial is used, the thinner or smaller extent the shock is resolved. A closer look on proposed shock capturing scheme implemented in the context of Discontinuous Galerkin method is performed in this article.

II. Shock capturing scheme

We are interested in solving the following equation of conservation law

$$\frac{\partial \mathbf{u}}{\partial t} + \nabla.\mathbf{F}(\mathbf{u}) = 0 \qquad (1)$$

over the domain Ω with the appropriate boundary condition and initial condition given as

$$\mathbf{u}(\mathbf{x}, t = 0) = \mathbf{u}_0(\mathbf{x}), \qquad (2)$$

where $\mathbf{u}$ is the conserved quantiy and $\mathbf{F}$ is the flux vector.

There are many approaches to deal with the problem involving discontinuities, shock waves and we are interested in using discontinuous Galerkin (DG) method to resolve these problems. In the context of DG method, it can be found in the literature that the solutions have to be limited if the shocks occur and there are a number of ways doing this limitation. In spite of the successful development over the years on the limiters used to handle the discontinuities in DGM, there are still a lot of problems which need to be investigated. While it is easily applicable and very well understood on how to limit the solutions in one dimensional cases, the problems in higher dimension are not yet well resolved.

A. Discontinuous Galerkin Method

Let $\mathcal{V}_h^p(\Omega)$ be the space of polynomials of degree p on the subdivision $\mathcal{T}_h$ of the domain Ω into elements $\Omega = \bigcup_{\kappa \in \mathcal{T}_h} \kappa$,

$$\mathcal{V}_h^p(\Omega) = \left\{ \mathbf{v} \in L^2(\Omega) : \mathbf{v}|_\kappa \in P^p(\kappa), \forall \kappa \in \mathcal{T}_h \right\}. \quad (3)$$

Discontinuous Galerkin formulation is expressed as follows: find $\mathbf{u}_h \in \mathcal{V}_h^p$ such that

$$\int_\kappa \mathbf{v}_h^T (\mathbf{u}_h)_t \mathrm{d}\mathbf{x} - \int_\kappa \nabla \mathbf{v}_h^T . \mathbf{F}(\mathbf{u}_h) \mathrm{d}\mathbf{x} + \int_{\partial \kappa} \mathbf{v}_h^T \hat{\mathcal{F}}(\mathbf{u}_h^+, \mathbf{u}_h^-) \mathbf{n} \mathrm{d}s$$
$$= 0, \qquad \forall \mathbf{v}_h \in \mathcal{V}_h^p, \quad (4)$$

where $\hat{\mathcal{F}}(\mathbf{u}_h^+, \mathbf{u}_h^-)$ is the numerical flux at interior element boundary or domain boundary. The $()^+$ and $()^-$ notations indicate the trace of solution taken from the interior and exterior of the element, respectively, and $\mathbf{n}$ is the outward normal vector to the boundary of the element. The numerical flux $\hat{\mathcal{F}}(\mathbf{u}_h^+, \mathbf{u}_h^-)$ can be taken as any Lipschitz continuous monotone flux, for example Roe's flux or Lax-Friedrichs flux.

B. Shock indicator

As the solution develops discontinuities, there must be a switch that allows one to turn on the limiter to resolve the discontinuities. In this case an indicator is designed to identify the trouble cells where the viscosity is added. The solution is expressed in term of p order orthogonal basis as

$$\mathbf{u} = \sum_{i=1}^{N(p)} \mathbf{u}_i \phi_i, \qquad (5)$$

where $\phi_i \in \mathcal{V}_h^p$, $i = 1, ..., N(p)$ are the basis polynomials. The orthogonal Legendre polynomials are used as basis functions in one dimension while an orthogonal Koornwinder basis [11] is employed for two dimensional triangulation elements. In general if the solution is smooth the coefficients decay very quickly while it is very slowly decaying for non smooth solution. In the case of Fourier expansion the Fourier coefficients

would decay with the rate of $1/k^{m+1}$ given that the function is m-order differentiable. We adopt the following smoothness indicator [12] which is defined within each element κ as

$$S_\kappa = \frac{(\mathbf{u} - \hat{\mathbf{u}}, \mathbf{u} - \hat{\mathbf{u}})_\kappa}{(\bar{\mathbf{u}}, \bar{\mathbf{u}})_\kappa}, \qquad (6)$$

where $(., .)_\kappa$ is the standard inner product in $L_2(\kappa)$, $\hat{\mathbf{u}}$ is the truncated expansion of the same solution containing the terms up to order $p - 1$,

$$\hat{\mathbf{u}} = \sum_{i=1}^{N(p-1)} \mathbf{u}_i \phi_i, \qquad (7)$$

with $\bar{\mathbf{u}}$ is the constant representative value of the solution. Essentially if the approximated solution is assumed to be continuous and the polynomial expansion behaves in a similar manner as the Fourier expansion then the coefficients would decay in the order of $1/k^2$. Therefore we expect that values of S_κ will scale like $\sim 1/p^4$.

C. Viscosity limiter

The proposed limiter uses the idea of viscosity for the numerical solution. Instead of flattening out the discontinuities or the employment of some high order non-oscillatory reconstruction, an appropriate amount of viscosity can be added in to spread the discontinuities over several cells such that it can be well resolved in the space of the interpolating polynomials. With the above mentioned indicator in previous section, one can detect in which elements the shock is located and the appropriate amount of viscosity is then added to resolve the discontinuity in the solution with continuous approximation. In order to do that a viscous term is added to the original equation as follows

$$\frac{\partial \mathbf{u}}{\partial t} + \nabla \cdot \mathbf{F}(\mathbf{u}) = \nabla \cdot \mathbf{F}_v(\mu, u, \nabla u) \qquad (8)$$

where μ is the amount of viscosity and $\mathbf{F}_v(\mu, u, \nabla u)$ is the viscous flux function. It can be clearly seen that the viscosity parameter μ is chosen as a function of the mesh size and order of approximating polynomials. In the region of shock as detected by the indicator the viscosity added to the model is taken to be proportional to $(\frac{h}{p})$ where p is the order of interpolation polynomials and h is the mesh size whereas no viscosity is used in the region of well resolved solution. A simple form of flux function which is commonly used is given in the form of $\mu \nabla \mathbf{u}$. A number of tests will be carried out to show that this simple model can give a very good result in some of the cases; for example, the Burgers' equation.

However in using viscosity to resolve the shock for Euler's system, a more complex flux function (in fact the physical one) is used to resolve the shocks. Hence using a constant, problem-independent value of viscosity to capture the shock with different strength will not give the expected answer due to the nonlinear behavior of the physical viscous flux. The viscosity added to the system must be set based on the problem nature. In the attempt to find the viscosity, it is physically motivated by the fact that for the Euler's system viscosity is

dependent on the temperature. There are a few expressions for the temperature dependent viscosity of which a commonly used is the formula of Sutherland,

$$\mu(T) = C\frac{T^{1/2}}{1 + T^*/T}, \quad (9)$$

where C and T^* are the constant. Another often used formula is given as

$$\frac{\mu}{\mu_0} = \left(\frac{T}{T_0}\right)^\alpha, \quad (10)$$

where μ_0 is the reference viscosity at the reference temperature T_0. The viscosity which is applied to each cell in the computational domain is determined by Equation (10).

It is noted that the standard DG method can not be applied to discretize the viscous term in the Equation (8) which involves high order derivative. The local discontinuous Garlerkin (LDG) method [1] is used to handle the second order derivative in the viscous flux function.

III. NUMERICAL APPLICATIONS

A. One dimensional applications

We first consider the scalar Burgers equation in one dimension

$$u_t + (\frac{u^2}{2})_x = 0 \quad (11)$$

in the domain [0,2] with smooth initial condition described as

$$u(x, t = 0) = a\sin(\pi x), \quad (12)$$

where a is the amplitude of the wave which characterizes the strength of the shock formed in the solution. Solution at t=$1.0/\pi$ is shown in Fig. 1 for $p = 10$ with the grid of 41 elements. This is a very simple test to check how the shock capturing scheme works. Starting with a sine wave, shock will gradually form and become stationary at $x = 1.0$, and the shock strength scales with parameter a. It can be seen that the shock is very well captured with a very high order method but reasonably coarse mesh. In this example we use the same amount of viscosity for different shock strengths and there is no oscillation found in the solutions. It can therefore be concluded that the viscosity added into the system is independent of the shock strength. This can be explained by the observation that in the scalar Burgers equation the viscous flux ($\mu\Delta u$) is always proportional to the change in the velocity u. As the velocity is increased, corresponding to the increase in shock strength, the viscous flux is scaled proportionally to insure that it can always revolve the shock.

Next we consider the Euler's equations in one-dimension

$$u_t + \nabla \cdot F_e(u) = 0, \quad (13)$$

where u are the conservative variables and $F_e(u)$ is the inviscid (Euler) flux function; these are

$$u = \begin{pmatrix} \rho \\ \rho u \\ \rho e \end{pmatrix} \qquad F_e(u) = \begin{pmatrix} \rho u \\ \rho u^2 + p \\ \rho h u \end{pmatrix} \quad .$$

The solution is initialized with an nonlinear isentropic acoustic wave given as

$$u = u_0 + \frac{2}{\gamma - 1}(a - \sqrt{\gamma})$$
$$\rho = 1 + c\sin(2\pi x)$$
$$p = \rho^\gamma$$

where u_0 is the velocity of the free stream with a pressure of $p_0 = 1$ and $\rho_0 = 1$, c is the amplitude of the wave. Basically the wave speeds are different at every point on the wave therefore the acoustic wave propagates and steepens to form the shock. Depending on the values of free stream velocity, the wave propagates at average speed of $(u_0 + \sqrt{\gamma})$. In this example, $u_0 = -\sqrt{\gamma}$ and a stationary shock is form after a period of time depending on the solution profile. To resolve the shock a viscous flux is added to the cell(s) which is found to contain the shock via Equation (6). The viscous flux could be artificial ($F_v(u) = \mu\nabla u$) or a physical one where

$$F_v(u, \nabla u) = \mu \begin{pmatrix} 0 \\ (2 + \lambda)u_x \\ u(2 + \lambda)u_x + \gamma/Pr e_x \end{pmatrix}.$$

In Figure 2, the density and mach number at time t=1.0 are shown for the case of $a = 0.15$. The shock is very well captured within 1-2 cells. Note that the viscosity will affect the stability of the method and we have to use a smaller CFL number to capture the shock. Applying the temperature dependent viscosity to capture the shock with different strength are shown in Figure 3 for $c = 0.6$ and 0.8. Note that for a higher value of amplitude c, the wave is no longer considered as linear. In these cases, the reference temperature is taken such that $p/\rho = 1$ and the corresponding viscosity is 1.0×10^{-3}. It can be seen that the shock in both cases are well resolved via the temperature-dependent viscosity.

Consider now the flow of compressible, idea gas through a variable-area channel governed by the quasi-1D Euler equations. The geometry of the channel is described as follows:

$$A(x) = \begin{cases} A_0, & x \le x_1 \cup x \ge x_2; \\ A_0 + (A_t - A_0)\left[cos\frac{\pi(x-0.5)}{x_2-x_1}\right]^2, & \text{otherwise.} \end{cases} \quad (14)$$

Here $A(x)$ is the cross section area along the channel. Depending on the geometry and the outflow condition (back pressure or Mach number), the flow in the channel can be isentropic subsonic or shocked transonic. In this case the area of the nozzle throat and exit Mach number are set such that there is a shock in the nozzle, the shock strength is dependent on the exit Mach number and the throat area. In Figure 4, the solutions of pressure and Mach number along the nozzle are shown for case examples of different throat areas and exit Mach numbers and hence shocks with different strengths will be formed in the nozzle. It can be seen that the shocks can be captured quite well for mentioned case examples of $A_t = 0.2, M_e = 0.5$ and $A_t = 0.025, M_e = 0.4$.

B. Two dimensional applications

For simplicity, we shall extend the acoustic problem in one dimension to two dimensions. The scheme is tested in 2D by considering the Euler equations in two dimensions with the flow conditions being extended from the simple acoustic wave problems presented in the previous section. Initial condition is the same as in the 1D problem with the velocity taken to be zero for the vertical component and periodic boundary condition is applied in y direction. The amplitude of the wave is taken as $a = 0.4$. The solution of density and Mach number are shown in the Figure 5 at time $t = 0.5$. It can be seen that the shock is resolved within almost one element and the scheme works for two dimensional problems.

Next we consider a flow over a bump of height h in the domain of $[0, 10] \times [0, 4.146]$. The bump on the upper half of a 4.2% circular arc of width 2 with the center located at $(5, 0)$. The problem is to compute the flow field in the domain within the range of transonic flow. In this example, the flow at $M = 0.85$ over the bump will be computed. Inflow boundary condition is applied on the left, with outflow conditions on the right and the top. At the bottom of the domain, solid wall boundary condition is applied. On the boundary conditions, the state value at the inflow/outflow boundaries is determined by using the outgoing Riemann invariants in the normal direction to the boundary and given boundary data. At the solid boundaries, a symmetric boundary condition is applied to specify the state condition which has the same density, internal energy and tangential velocity as the internal components and opposite normal velocity.

The solution of the pressure and Mach number are shown in the Figure 6. In this coarse grid of 192 elements refined in the region closed to the bump surface the shock is reasonably resolved within to about one element. The computation should be performed until the steady state solution is obtained based on a tolerance of 10^{-3} for the norm of density residual.

IV. CONCLUSION

It has been shown that viscosity term can actually resolve the shock in the context of discontinuous Galerkin method. With the appropriate amount of viscosity added into the system the discontinuities in solution can be spread out in the band of several cells in the domain and very well approximated by the interpolating polynomials. While a constant amount of viscosity can resolve the shocks with expected resolution in the case of scalar problem with linear viscous term, it has to be scaled with the solution profiles in order to approximate the shock better in the non-linear case; for example for the Euler equations which the viscosity is taken to be proportional to the flow temperature. Both one and two dimensional problems are tested and show that the proposed approach is capable of capturing the shocks and discontinuities. For the two dimensional problems, the shock is well resolved by the temperature-dependent viscosity term. However there remains some issues relating to stability in the present employment of explicit method. Future direction is to incorporate an implicit time-stepping scheme to permit reasonably large time step.

REFERENCES

[1] Bernardo Cockburn and C.-W. Shu, *Runge-Kutta Discontinuous Galerkin Methods for Covective-Dominated Problems*, Review Article, J. Sci. Comp., v16 (2001), pp.173-261.

[2] Bernardo Cockburn and C.-W. Shu, *TVB Runge-Kutta local projection discontinuous Galerkin finite element method for conservation laws II: General framework*, Math. Comput., v52 (1989), pp.411.

[3] Bernardo Cockburn and C.-W. Shu, *TVB Runge-Kutta local projection discontinuous Galerkin finite element method for conservation laws III: One dimensional systems*, J. Comput. Phys., v84 (1989), pp.84.

[4] Bernardo Cockburn and C.-W. Shu, *TVB Runge-Kutta local projection discontinuous Galerkin finite element method for conservation laws IV: The multidimensional case*, Math. Comput., v54 (1990), pp.545.

[5] Bernardo Cockburn and C.-W. Shu, *TVB Runge-Kutta local projection discontinuous Galerkin finite element method for conservation laws V: Multidimensional Systems*, J. Comput. Phys., v141 (1998), pp.199-224.

[6] J. Qiu and C.-W. Shu, *Runge-Kutta discontinuous Galerkin method using WENO limiters*, SIAM Journal on Scientific Computing, v26 (2005), pp.907-929.

[7] J. Qiu and C.-W. Shu, *A comparison of troubled cell indicators for Runge-Kutta discontinuous Galerkin methods using WENO limiters*, SIAM Journal on Scientific Computing, to appear.

[8] F. Bassi and S. Rebay, *High order accurate discontinuous finite element solution of the 2D Euler equations*, J. Comput. Phys., v138 (1997), pp.251-285.

[9] R. Biswas, K. D. Devine and J. E. Flaherty, *Parallel, adaptive finite element methods for conservation laws*, Appl. Numer. Math., v14 (1994), pp.255-283.

[10] J. Von Neumann and R. D. Richmyer, *A method for numerical calculation of hydro dynamic shocks*, J. Appl. Phys., v21 (1950), pp.232-237.

[11] Tom H. Koornwinder, *Askey-Wilson polynomials for root systems of type BC*, Comptemp. Math., v138 (1992), pp.189-204-237.

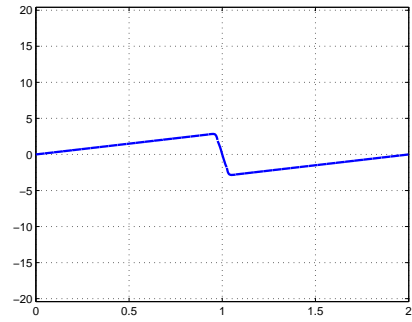[12] P.-O. Persson and J. Peraire, *Sub-cell shock capturing for discontinuous Galerkin methods*, Manuscript, 2005.
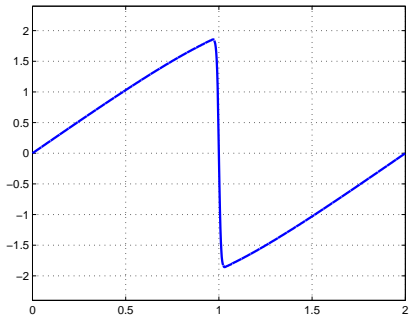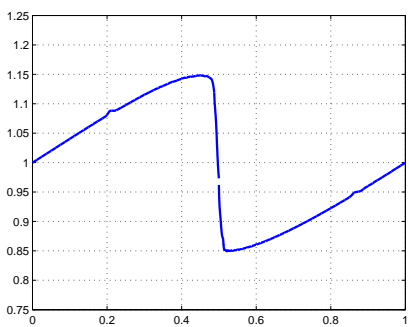
(a) a=2.0
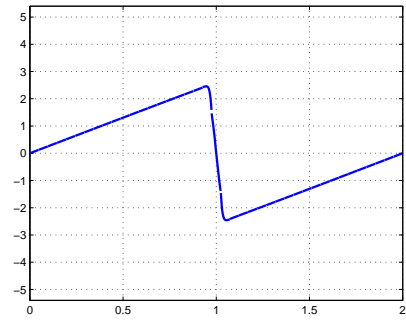
(b) a=5.0
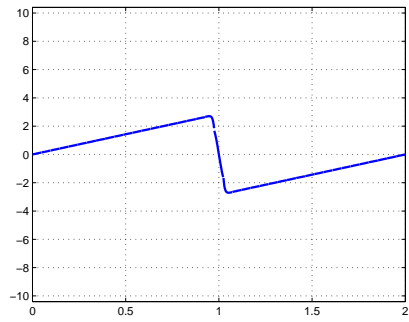
(c) a=10.0

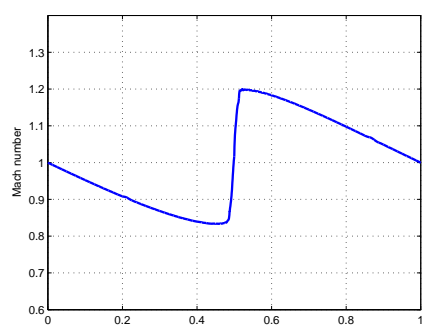(d) a=20.0

Fig. 1. Burgers equation's solution at t=1/π, $p = 10$, 41 elements: (a) a = 2; (b) a = 5; (c) a = 10; (d) a = 20. The shocks are very well resolved in one element. Figures are not on the same ordinate scale.

(a) Density

(b) Mach number

Fig. 2. Euler equations, density and Mach number profile at $t = 1.0$ for $c = 0.15$, temperature dependent viscosity. The shock is formed from the acoustic wave and resolved in 2 cells.
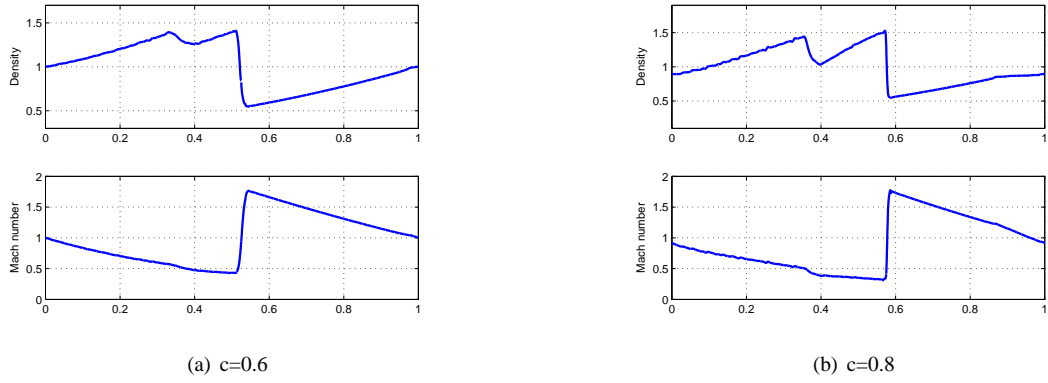
(a) c=0.6

(b) c=0.8

Fig. 3. Shock capturing, solution for $c = 0.6$ (top) and $c = 0.8$ (bottom) at t=0.4, $p = 5$. Note how the different strength shocks are resolved by using the temperature dependent viscosity.
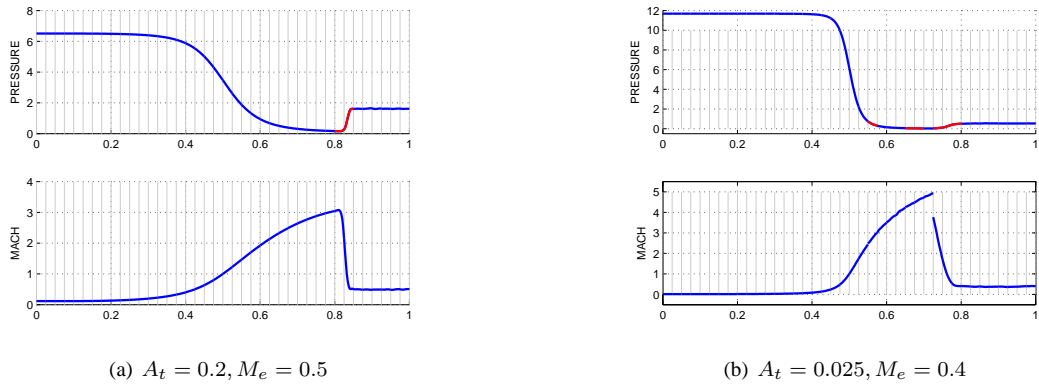

(a) $A_t = 0.2, M_e = 0.5$

(b) $A_t = 0.025, M_e = 0.4$

Fig. 4. Nozzle flow, solutions of pressure and Mach number with different nozzle configurations at t=1.0, $\mu_0 = 1.0 \times 10^{-3}$. Note at the jump in the Mach number in the shock region.
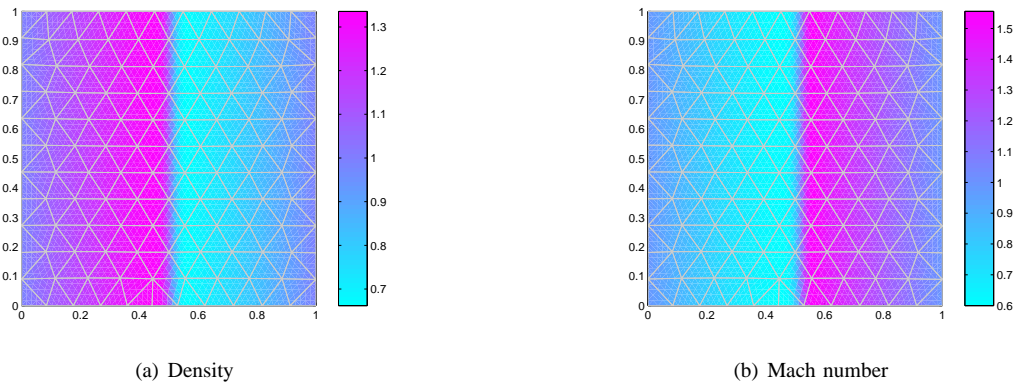

(a) Density

(b) Mach number

Fig. 5. Two dimensional Euler problem, shock formed from sine wave. Using $P = 4$, density and Mach number shown at t=0.5. The shock is almost resolved within 1 element.
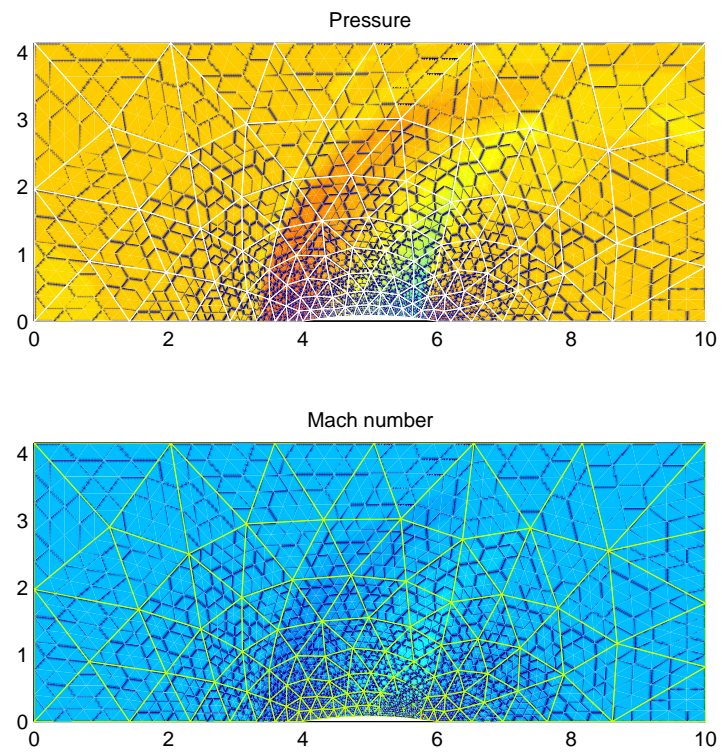
Fig. 6. Two dimensional inviscid compressible flow over a bump. Solutions of pressure and Mach number are shown with $p = 4$. The shock is almost resolved within 1 element.